THE INFLUENCE OF MATERIAL PROPERTIES ON ROTARY DRAW BENDING PROCESSES

Prof. Dr.-Ing. B. Engel[1)], M.Sc. H. Hassan[1,2)*]

1)   Chair of Forming Technology, University of Siegen, 57076 Siegen Germany
2)   University of Baghdad, Bagdad Iraq
*Corresponding author: Hassan Raheem Hassan; e-mail: Hassan.Hassan@uni-siegen.de

ABSTRACT

Rotary draw bending is a method that is used in tube forming. In the tube bending process, the wall thickness distribution changes for the tube's cross section because the neutral axis moves towards the inner arc. Thinning takes place in the outer arc of the tube due to the stretching of the material, whereas thickening occurs in the inner arc of the tube due to the compression of the material. This paper investigates in the rotary draw bending process with different material properties (steel alloy 1.0036 and stainless steel alloy 1.4301). FE-simulation and experimental tests are employed to calculate the variable characteristics such as wall thinning / thickening, neutral axis shifting and strain distribution. The research is compared with the theoretical calculations. The theoretical model is based on a geometrical model that was presented in a previous work. This study helped us to identify the influence of the material properties on rotary draw bending.

Index Terms - Rotary draw bending, neutral axis shifting, wall thickness distribution, strain distribution, Material influence.

1.   INTRODUCTION

Due to its high forming advantages, the NC bending process of thin-walled tubes has been attracting more and more applications in aerospace, aviation, automobile and various other high technology industries as well as it has also been satisfying the increasing needs for high strength / weight ratio products. The technology has become one of the main fields in the research and development of advanced plastic forming technology [2].

Figure (1a) shows a sketch of the rotary draw bending process. The tube is inserted into the bending machine and clamped between the inner and the outer clamp die. By the rotation of both (inner clamp die and outer clamp die) around the bending axis, the tube is formed according to the radius of the bending die. The pressure die (slide piece) serves the purpose of taking up the radial stress, which is generated during the forming process and supports the straight tube end from the outside. If a mandrel and a wiper die are applied additionally (mandrel bending), high work piece quality can be achieved even with thin-walled tubes and small bending radii [3]. The geometry of the tube and the tube's cross section after bending are shown in the figures (1b) and (1c). The original neutral axis of the tube is denoted in the center of the tube and the distance from the center of the tube to the center of the bending die is called bending radius (R_b). The neutral axis is moved towards the inner arc. The distance between the center of the bending die and the shifted neutral axis is called (R`). The wall thickness distribution of the tube's cross section is characterized by the thinning that took place in the outer arc of the tube (t_{out}) and the thickening that occurred in the inner arc of the tube (t_{in}).
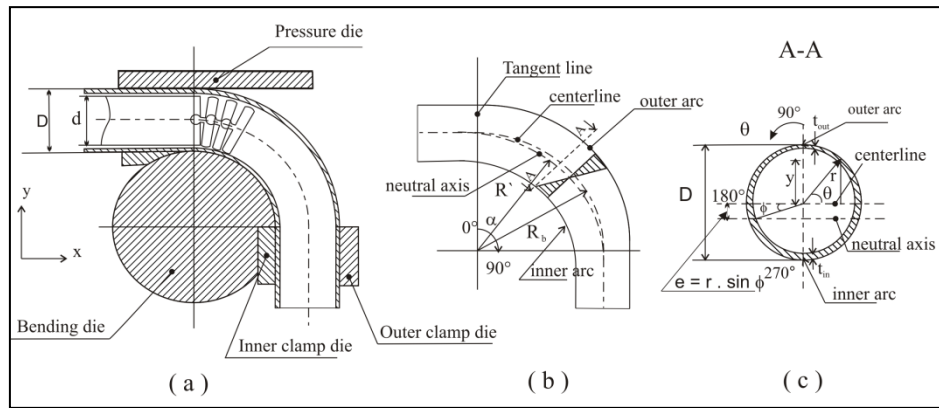
Figure (1): Tools for the rotary draw bending process and typical wall thickness distribution

Many of the researchers on rotary draw bending processes use different parameters such as springback, one material, deflection in the tube after bending and stress-strain distribution, and several researchers focus on neutral axis shifting in experimental tests as well as on FE simulation. These researches are useful to understand the bending in rotary draw bending processes. H. Li et al. [4] studied the wrinkling, wall-thinning cross section deformation and developed an analytical description. The deformation behaviors of thin-walled tube NC bending with large diameters D/t (50.0-87.0) and small bending radii Rd/D (1.0-2.0) are explored by a series of 3D-FE models using ABAQUS. M. Zhan et al. [5] developed the rigid-plastic finite element method (FEM) based on a principle in which a three dimensional (3D) rigid-plastic FE simulation system named TBS-3D (tube bending simulation by 3D FEM) is used for the NC bending process of thin-walled tubes, and a reasonable FEM model is established. NC bending processes of thin-walled tubes are simulated by using this FE simulation system, In addition, the stress distribution is obtained along the bending direction. L.Sözen et al. [6] studied the springback phenomena involving interactions between the geometrical and mechanical parameters. This model is developed by finite element analysis using the multi-purpose explicit and implicit finite element software "Ls-DYNA" to analyze the non-linear response of structures.

In this study, the experimental tests show the influence of material properties on each of the wall-thinning / thickening, neutral axis shifting and strain distribution. In addition, an FE simulation of the rotary draw bending has been developed and compared with the results obtained from using the experimental tests as well as the theoretical calculations. Theoretical calculations in tube bending based on a geometrical model were presented by [1] "In the previous work, we determined the magnitude of the neutral axis shifting, the wall-thinning / thickening and the axial strain distribution based on geometry shape of the tube cross section, the bending radius and the bending angle".

2. EXPERIMENTAL PROCEDURE

2.1 Rotary draw bending processes

In this work, the bending tests are carried out using a CNC bending machine that was produced by the Tracto-Technik GmbH & CO.KG Company. This machine has been specially designed to be used in rotary draw bending and also for free-form bending, see figure (2).

Figure (2): Rotary draw bending machine TT120UTS

The bending machine is equipped with special parameters for this work, see table (1). The rotary draw bending tools include the bending die, clamp dies, the pressure die, the wiper die and a universal flexing mandrel with four mandrel balls. The experimental test was carried out at room temperature. The friction coefficient is (0.1) along the tube-tools interfaces (except the friction between the tube and the clamp dies, which is (0.27)). The lubrication oil is used as an antifriction material between the mandrel and the internal wall of the tube.

Table (1): Dimensions of the tools

Parameters	Values
R_b	75 mm
L_c	40 mm
L_p	300 mm
L_w	140 mm
F_p	45 kN
F_c	70 kN
W (Wall Thickness Factor)	20
B (Bending Factor)	1.87
D	40 mm
t_o	2mm

2.2   MECHANICAL PROPERTIES

The mechanical properties of the tube are obtained from the uniaxial tensile test. The rectangular specimen is used for these tensile tests. The characteristic material values are yield strength $R_{p0,2}$, tensile strength R_m and uniform elongation A_g, which are all determined by tensile tests. These values are obtained from the values of three tensile specimens. The average mechanical properties are shown in table (2). Figure (3) depicts the stress-strain curves of the tube material obtained from a tensile test.

Table (2): Mechanical properties of stainless steel alloy 1.4301, steel 1.0036

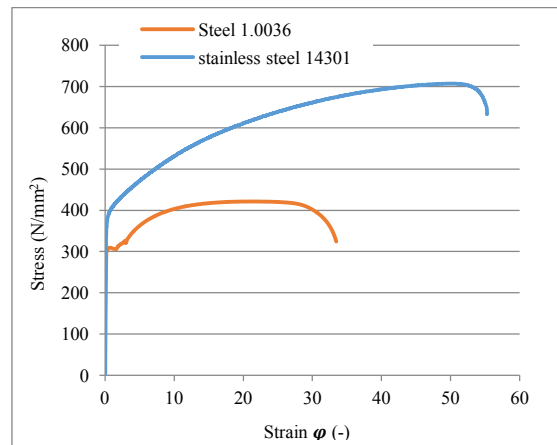| Parameters	Stainless steel alloy (1.4301)	Steel alloy (1.0036)
Young's modulus, E (GPa)	195	210
Poisson's ratio, ν	0.3	0.3
Density, ρ (g/cm3)	7.86	7.85
Strain Hardening exponent, n	0.37	0.1906
$R_{p0.2}$ (MPa)	464	302.87
R_m (MPa)	707	417.32
A_g (%)	45	21. 28

Figure (3): The stress-strain curve obtained from a tension test.

2.3   Methods of Measurement

2.3.1   Strain Measurement

In the experimental test, the VIALUX device was used to measure the strain distribution of the tube. Full-field strain analysis done after the forming process is based on the measurement of initially squared grid patterns. This means that the workpiece metal has to be marked before forming. For that purpose, there are standard grid stencils with 1.0- 2.0mm. The grids are well optimized and enable fully automated evaluation of the forming state in many applications. Electrolyte is suited for the electro-chemical marking. In addition, VIALUX also supplies the electrical equipment that is necessary for marking. Figure (4) shows the results obtained from FLC and the grid on the tube.
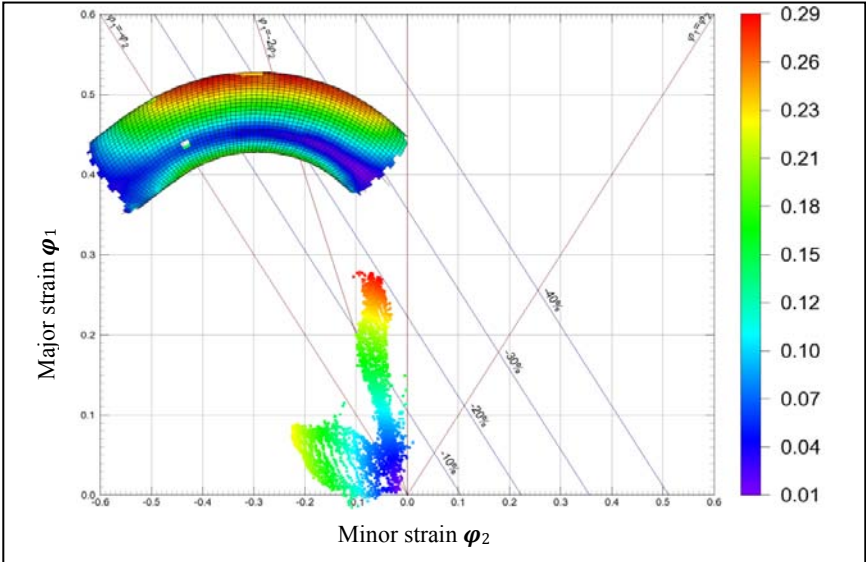
Figure 4: FLC result and the grid on the tube

2.3.2 Wall Thickness Measurement

The wall thickness measuring device was used to measure the wall thickness of the tube. It consists of a calliper with an inductive sensor. The sensor signal is measured and converted by a computer-integrated A/D converter card with a 16 bit resolution. The high-resolution A / D converter provides a resolution of the electric field in the wall thickness of 0.6 μm. With careful calibration, an absolute accuracy can be achieved up to a value of about ± 5 μm or more. The wall thickness measuring device is competent with the requirements of the experimental precision, see figure (5).

The wall thickness changing is calculated from the following equation:

$$Wall\ thickness\ changing\ (\%) = \frac{t_{new} - t_o}{t_o} .100\ \%$$ ………………………………………………..……..……….. (1)

Where, t_o is the original wall thickness, t_{new} is the wall thickness after bending. Hence, the wall thickness changes (%) are negative in the outer arc and positive in the inner arc.
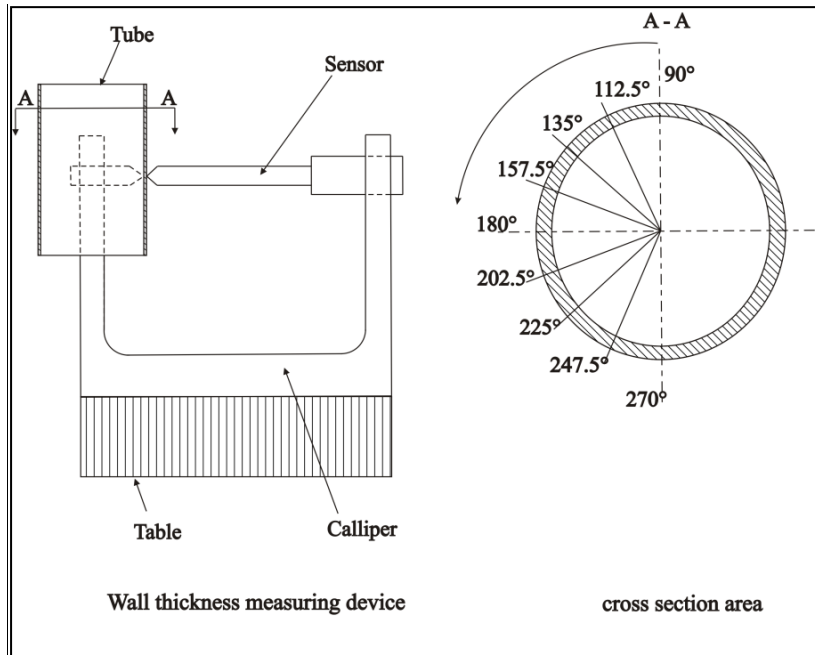
Figure (5): Sketch of the wall thickness measuring device

3 FINITE ELEMENT ANALYSIS

Finite element models of rotary draw bending were performed in the program "PAM-TUBE" to predict the wall thickness distribution, the maximum strain distribution and the neutral axis shifting towards the inner bow of the tube. The finite element models comprise the tube, tools, boundary constraints and material properties [1].
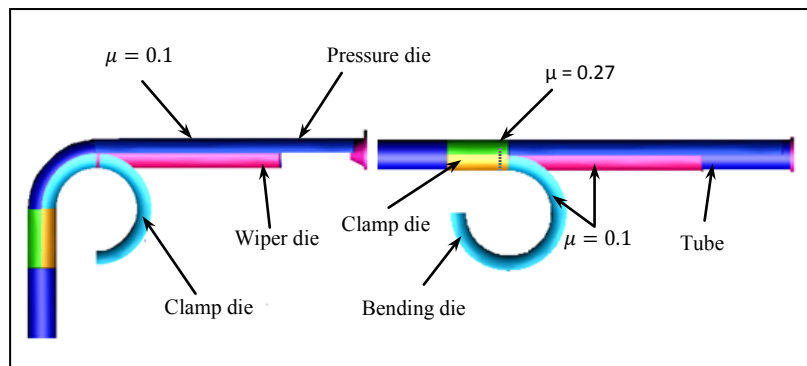

Figure (6): Finite element model for the rotary draw bending

Figure (6) shows the finite element model for rotary draw bending. The tools include the bending die, the clamp dies, a pressure die, a wiper die and a universal flexing mandrel with four mandrel balls. The friction coefficient is (0.1) along the tube-tools interfaces except between the tube and the clamp dies where it is (0.27). In table (1), the values for the dimensions of the tools and process parameters that were used in the finite element model are shown: R_b is the bending radius, L_c is the length of the clamp die, L_p is the length of the pressure die, L_w is the length of the wiper die, W is the wall thickness factor (ratio of the tube's outside diameter to the wall thickness, $W = D/t_o$), B is the bending factor (ratio of the bending radius to the tube's outside diameter, $B = R_b/D$), F_p is the pressure force, F_c is the clamp force, D is the diameter of the tube and t_o is the original wall thickness.

The shell elements of the Belytscho-Tsay type are used in the Finite Element Model. The Belytscho-Tsay element is a simple and efficient element that is based on the concept of a uniform and reduced integration. The Belytscho-Tsay element with four points is used for the meshing in the mid surface of the tube [1].

During the finite element simulation in the rotary draw bending process, the tubes were made from two materials (stainless steel 1.4301 and steel 1.0036); material properties used in the simulations are given in table (2).

4 RESULTS AND DISCUSSION

The material properties have an influence on the tube wall thinning / thickening, the neutral axis shifting and the strain distribution. The FE simulation of the rotary draw bending process is carried out using the software "PAM-Tube". The experimental test and the FE-simulation results are compared with the geometrical model that was presented in a previous work.

4.1 Neutral Axis Shifting

The neutral axis shifting for different bending angles was calculated using FE-simulation as well as experimental tests and geometrical models for different materials (steel alloy 1.0036 and stainless steel alloy 1.4301) at a bending radius of 75mm with a wall thickness of 2mm. Figure (7) shows that the values of the neutral axis shifting using the experimental tests are closer to the FE-simulated results than the values using the geometrical model. The FE simulation and experimental test show that the neutral axis shifting is influenced by material properties. In comparison, the geometrical model shows constant values for different material properties.
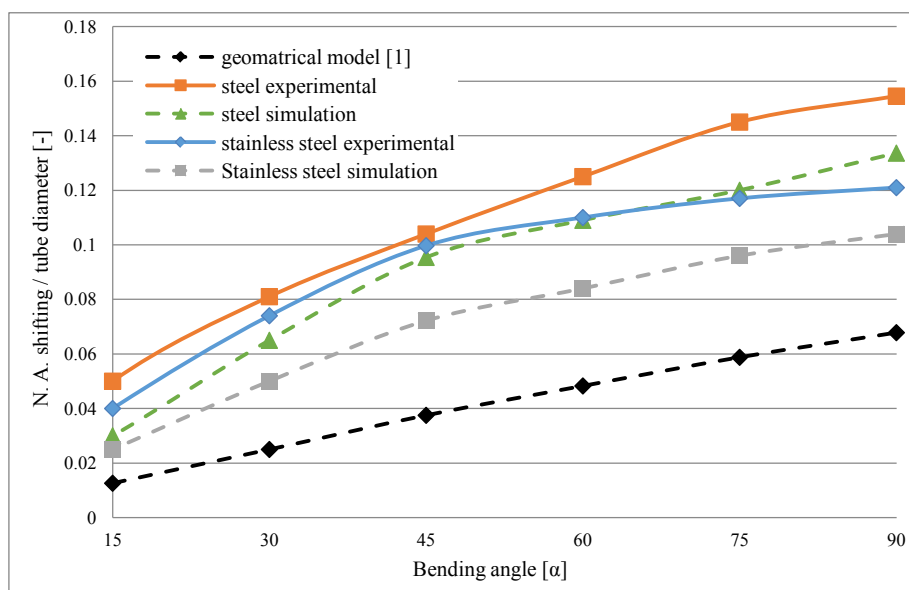

Figure (7): Neutral axis shifting with different bending angles

4.2 Wall Thickness Distribution

The wall thickness distribution is influenced by the material properties and the neutral axis shifting as well. As illustrated in figure (8) and figure (9), the distribution of the wall thickness in the tube's cross section was in the middle of the bend at a bending angle of 90°. It can be seen in figure (8) and figure (9), that the wall thickness is thinner in the extrados and thicker in the intrados due to tension and compression, respectively. The results from the FE-simulation and the experimental test were agreed in those figures. Figure (8) shows the change in the wall thickness with a stainless steel tube and figure (9) shows the change in the wall thickness with a steel tube. In addition, the wall thickness is influenced by the bending angles due to the stretch in the extrados and the compression in the intrados of the tube; see figures (10) and (11).
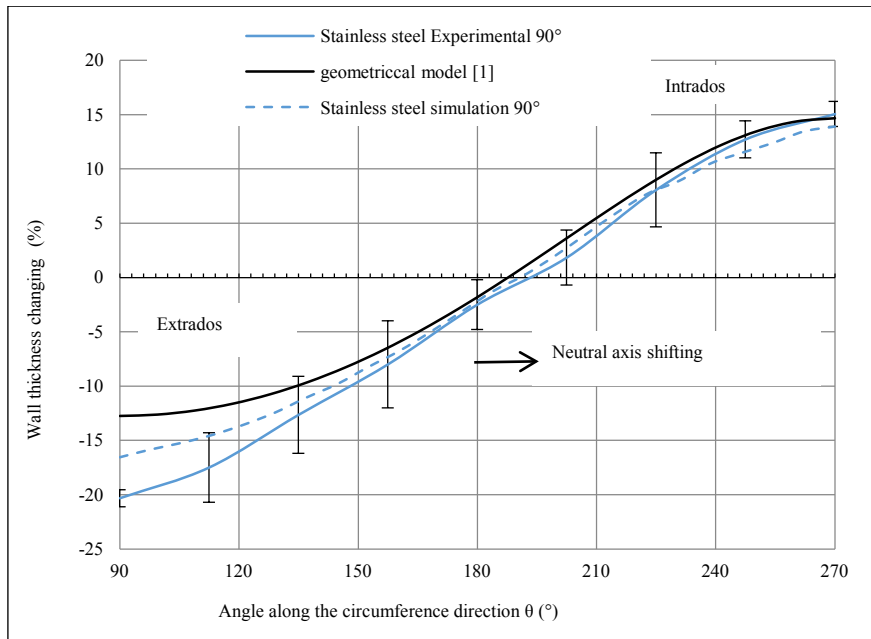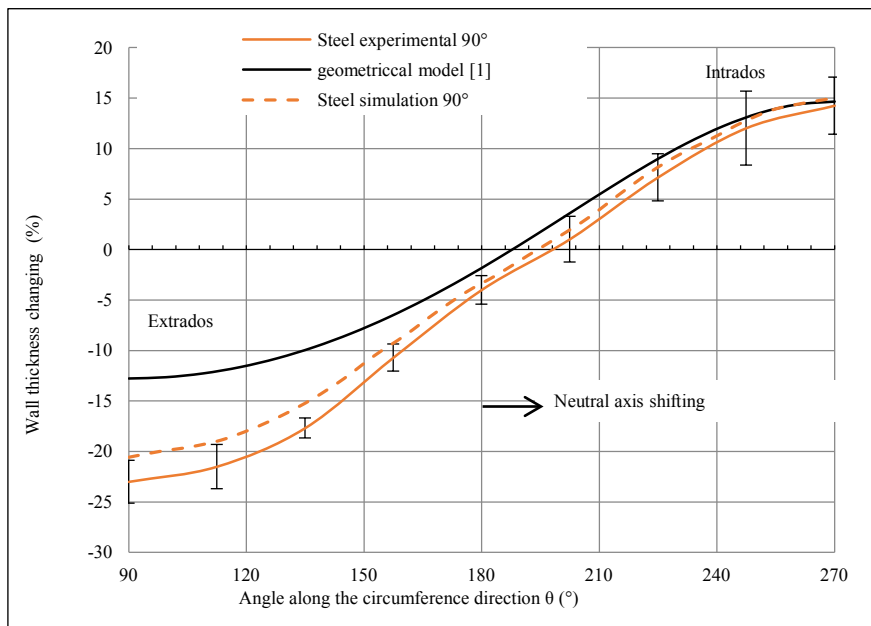
Figure (8): Comparison of the wall thickness distribution in the cross section of the tube obtained by using the geometrical model [1], the FE simulation and the experimental test for stainless steel alloy (in the middle of the bend, bending angle of 90°)

Figure (9): Comparison of the wall thickness distribution in the cross section of the tube obtained by using the geometrical model [1], the FE simulation and the experimental test for steel alloy (in the middle of the bend, bending angle of 90°)
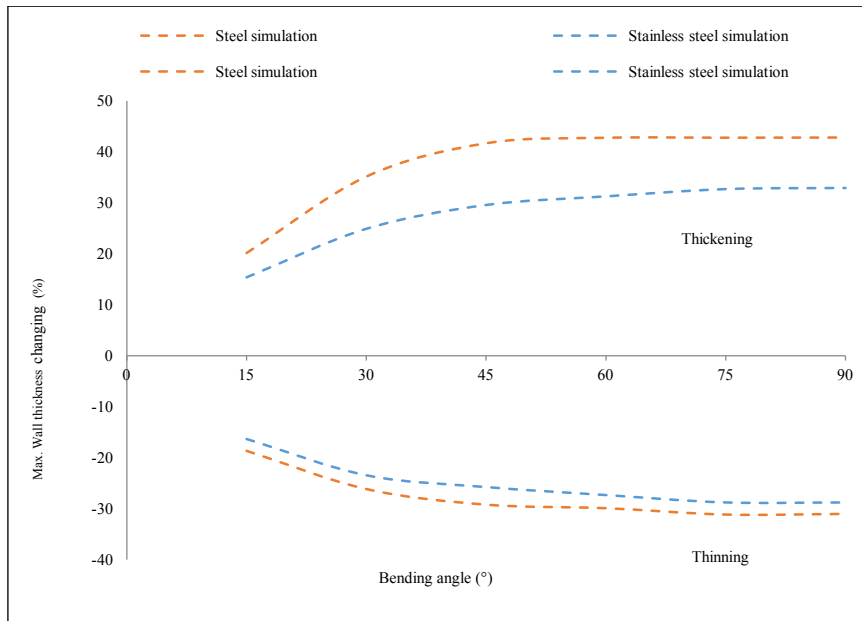
Figure (10): Max. wall thickness value with different bending angles using the FE simulation for stainless steel alloy and steel alloy at half bending angles
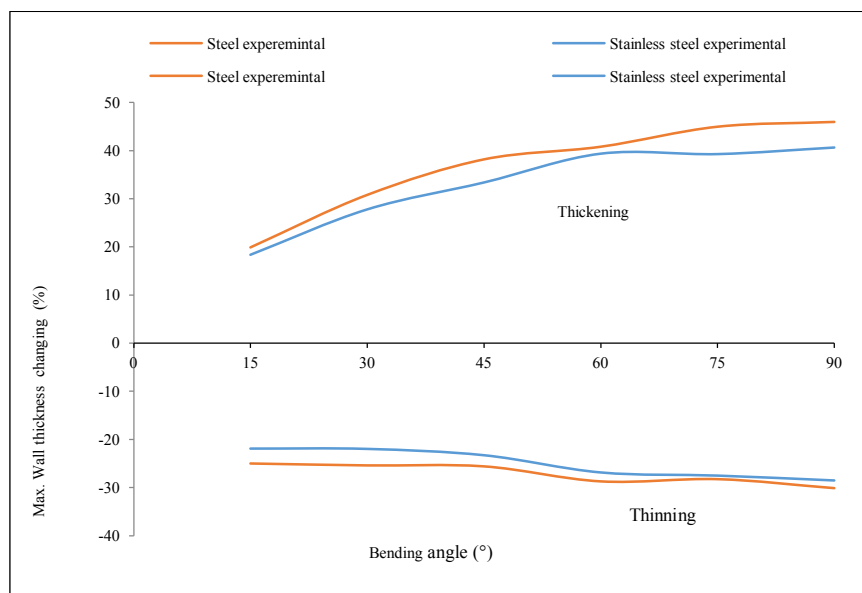

Figure (11): Max. wall thickness value with different bending angles using the experimental test for stainless steel alloy and steel alloy at half bending angles

4.3 Strain Distribution

The neutral axis shifting and the bending angle have influenced the strain distribution. Figures (12) and (13) show the longitudinal strain distribution based on the geometrical model [1], the FE simulation and the experimental test in the outer arc that were calculated from the starting angle (bending angle of 0°) to half the angle of the bend. Moreover, the material properties have influenced the strain values as explained in the figures. By using FE simulation and experimental tests, it could be found out that the strain distribution is higher for steel tubes than for stainless steel tubes due to stress- strain behavior.
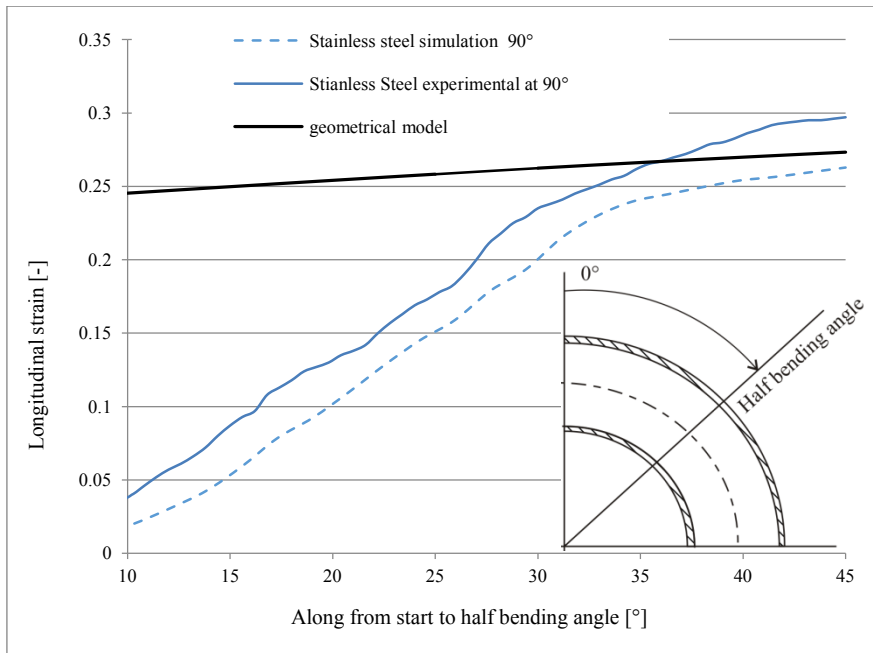
Figure (12): The longitudinal strain of the tube (from start to half angle of bend) using geometrical model [1], FE simulation for stainless steel alloy, and experimental test for stainless steel alloy (bending angle of 90°)
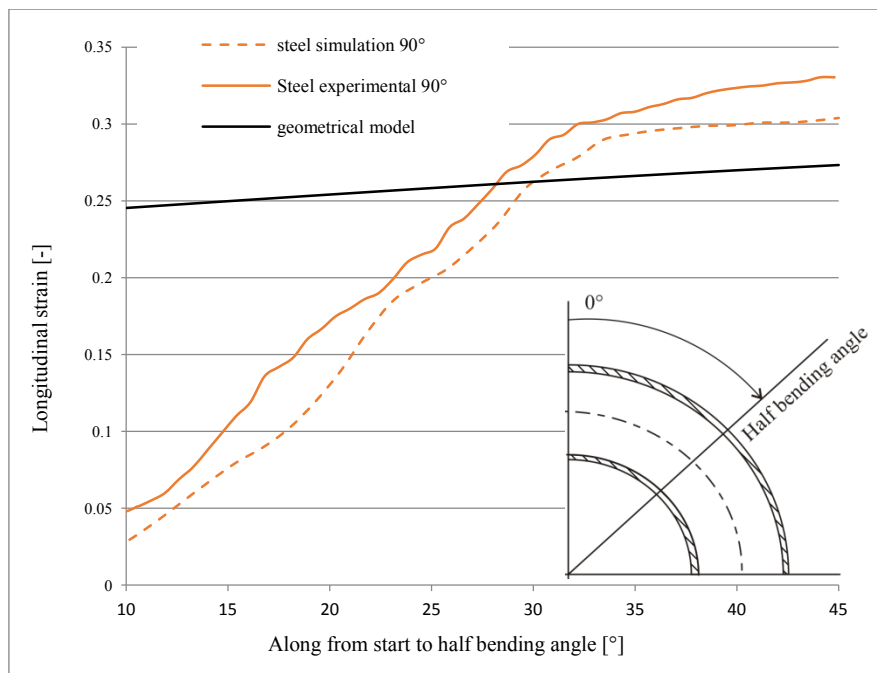

Figure (13): The longitudinal strain of the tube (from start to half angle of bend) using geometrical model [1], FE simulation for steel alloy, and experimental test for stainless steel alloy (bending angle of 90°)

5 CONCLUSIONS

In this paper, the influence of material properties on the neutral axis shifting, wall thickness distribution and the longitudinal strain in the rotary draw bending process have been studied. The experimental tests and the FE simulation have presented the calculation for the neutral axis shifting, wall thickness distribution and longitudinal strain. Comparing the results with (our) previous work [1], the conclusions are as follows:

- the material properties have an influence on the neutral axis shifting. The neutral axis of the tube moves more towards the inner tube in steel alloy than in stainless steel tubes. Furthermore, the material properties have an influence on the wall thickness distribution.

- the longitudinal strain in the outer arc of the tube is obtained from the experimental tests and the FE simulation. These results have been compared with the geometrical model [1]. It is shown that the longitudinal strain is influenced by the material properties and the neutral axis shifting.

ACKNOWLEDGMENT

REFERENCE

[1] Engel, B., Hassan, H. (2014), Investigation of Neutral Axis Shifting in Rotary Draw Bending Processes for Tubes. Steel research int..

[2] H. Yang, Z.C. Sun, Y. Lin, M.Q. Li, Advanced plastic processing technology and research progress on tube forming, Journal of Plasticity Engineering 8 (2) (2001) 86–88.

[3] Brewster, K., Sutter, K., Ahmetoglu, M.A., and Altan, T., 1996, "Hydroforming Tube," The Tube and Pipe Quarterly, **7**(4), pp. 34-40.

[4] H. Li, H. Yang, J. Yan and M. Zhan: Numerical study on the deformation behaviors of thin-walled tube NC bending with large diameter and small bending radius. In, computational material science 45 (2009) 921-934.

[5] M. Zhan, H. Yang, Z. Jiang, Z. Zhao and Y. Lin: A study on a 3D FE simulation method of the NC bending process of thin-walled tube. In, Journal of material processing technology 129 (2002) 273-276

[6] L.Sözen, M. Guler, D. Bekar and E. Acar: springback in rotary-draw tube bending process using finite element method. In, Journal of mechanical engineering science (2012).